Journal of Materials Chemistry C

ROYAL SOCIETY OF CHEMISTRY

PAPER

View Article Online
View Journal | View Issue



Check for updates

Cite this: J. Mater. Chem. C, 2022, 10, 9823

# Polythiophene-mediated light modulation of membrane potential and calcium signalling in human adipose-derived stem/stromal cells†

Ilaria Abdel Aziz,‡§[ab] Leonardo Maver,§[ab] Chiara Giannasi,[cd] Stefania Niada,[d] Anna T. Brini ¶*[cd] and Maria Rosa Antognazza ¶*[a]

Received 7th April 2022,
Accepted 5th June 2022

DOI: 10.1039/d2tc01426b

rsc.li/materials-c

Recent progress in the fields of regenerative medicine and tissue engineering has been strongly fostered both by the investigation of crucial cues, able to trigger the regeneration of damaged tissues, and by the development of *ad hoc* functional materials, capable of selectively (re-)activating relevant physiological pathways. In parallel to the successful realization of biochemical cues and the optimization of delivery protocols, the use of biophysical stimuli has been emerging as an alternative, highly effective strategy. Techniques based on electrical, magnetic and mechanical stimulation have been reported to efficiently direct differentiation of stem cells and modulate cell physiology at different developmental stages. In this framework, the use of optical stimulation represents a valuable approach, possibly overcoming current limitations of chemical cues, like limited spatial and temporal resolution and poor control over the extracellular environment. Surprisingly, the effects of light on the physiological properties (light toxicity, cell membrane potential, and cell ionic trafficking) of undifferentiated cells, as well as on their differentiation pathways, were investigated to a very limited extent and rarely quantified in a systematic way. In this work, we aim at clarifying the effects of optical excitation on the physiological behaviour of undifferentiated human adipose-derived stem cells (hASC), cultured on top of a light-sensitive conjugated polymer, region-regular poly-3-hexyl-thiophene (P3HT). Interestingly, we observe statistically significant modulation of the cell membrane potential, as well as noticeable effects on intracellular calcium signalling, triggered by P3HT excitation upon green light stimuli. Possible mechanisms involved in the signal transduction pathways are considered and critically discussed. The capability to modulate the physiological response of hASC upon photoexcitation, in a highly controlled and selective manner, provides a promptly available and non invasive diagnostic tool, thus contributing to the understanding of the complex machinery behind stem cells and material interfaces. Moreover, it may open the route to novel techniques to drive the differentiation path with unprecedented versatility and operational easiness.

## 1. Introduction

Human mesenchymal stem/stromal cells (MSC) represent a valuable tool for regenerative medicine, tissue engineering and cell therapy, due to their ability to differentiate into several cell types and to influence resident cells by paracrine mechanisms.[1] In particular, adipose-tissue derived stem cells (ASC) share very similar characteristics with stem cells derived from bone marrow, but they are much easier to recover and to expand.[2] Therefore, over the years hASCs became one of the most employed cell sources in regenerative medicine, mostly for bone and cartilage regeneration.[3,4] Extensive literature reported effective protocols for differentiation of human ASC (hASC) into adipocytes,[5] chondrocytes,[6] and osteoblasts.[7] Interestingly, hASC can also differentiate into excitable cells, *e.g.*, neurons[8] and cardiomyocytes.[9] To this goal, appropriate

[a] *Center for Nano Science and Technology@PoliMi, Istituto Italiano di Tecnologia, via Giovanni Pascoli 70/3, 20133 Milano, Italy. E-mail: Mariarosa.antognazza@iit.it*
[b] *Politecnico di Milano, Dip.to di Fisica, P.zza L. da Vinci 32, 20133 Milano, Italy*
[c] *University of Milan, Department of Biomedical, Surgical and Dental Sciences, Via Vanvitelli 32, 20129 Milano, Italy. E-mail: Anna.brini@unimi.it*
[d] *IRCCS Istituto Ortopedico Galeazzi, Via Galeazzi 4, 20161 Milano, Italy*

† Electronic supplementary information (ESI) available: Fig. S1: hASC characterization; Fig. S2: biological replicas of calcium imaging experiments; Fig. S3: biological replicas of calcium imaging experiments in calcium-free medium. Details about the protocol to evaluate cell responsivity. See DOI: https://doi.org/10.1039/d2tc01426b

‡ Current address: Laboratory of Organic Electronics, Linköping University, Bredgatan 33, 602 21 Norrköping, Sweden.
§ These authors contributed equally.
¶ Co-corresponding and co-last authors.

differentiation protocols and media with *ad hoc* chemical agents' composition have been developed and optimized. Though reliable and effective, such protocols require either the physical presence of an operator or an expensive automated sterile system for timely administration of drugs at fixed time points and follow up. Most importantly, differentiation protocols based on chemical cues are obviously irreversible and they completely lack spatial resolution, making the targeting of specific cell sub-populations within the same *in vitro* culture impossible. More effective strategies would require the control of the extracellular environment in a dynamic way, being able to provide selected stimuli at different time-points in a more versatile way. These limitations and requirements prompted researchers to investigate the opportunity to use biophysical cues, rather than biochemical ones, for effective and spatio-temporally controlled differentiation of stem cells.[10,11] Most approaches reported so far for directing MSC differentiation processes include electrical,[12–14] magnetic,[15,16] and mechanical[11] stimulation. Besides other physical stimuli, the use of optical stimulation has been attracting increasing attention in the latest few years.[17] Light offers distinctive advantages, such as minimal invasiveness and spatio-temporal resolution. Furthermore, it is possible to finely tune other parameters, including light density, wavelength, illuminated area, *i.e.* spatial and temporal patterning, that puts into practice the concept of '4D patterning'. Some recent examples of photonics approaches include the opportunity to change the mechanical properties of light-sensitive scaffolds,[18] or also to use photo-cleavable biochemical cues, which release the drug only when activated by light, in a temporally and spatially controlled manner.[19]

Independently of the differentiation induction stimulus (chemical or physical), however, the link between the stimuli characteristics, their impact on the cell physiology, and the possible modulation of the differentiation path remained in most cases quite elusive. The effect of electromagnetic stimulation on the physiological properties (light toxicity, cell membrane potential, and cell ionic trafficking) of undifferentiated cells was investigated to a very limited extent, and the origin of the possible effects on differentiation was rarely clarified. Even more, very limited consideration has been devoted, so far, to combining the advantages of electrical and optical stimulation in the field of regenerative medicine, through the selection of suitable light sensitive and photo-electrically active functional materials.[20–24]

In this work, we originally explore this possibility, by employing a prototype semiconducting polymer, namely regio-regular poly-3-hexyl-thiophene (P3HT), characterized by optimal cytocompatibility, excellent photostability, and good photoconduction properties in an aqueous environment.[25,26] In particular, we explore the possibility to modulate the physiological response of hASC upon photoexcitation, as a first preliminary step towards the creation of novel tools for driving the differentiation path with unprecedented versatility and operational easiness. We focus the attention on two main physiological properties, namely the modulation of the cell membrane potential and the capability to affect $Ca^{2+}$ ion dynamics. Both processes have been reported to be linked with the differentiation pathways of hASC. The effective use of light stimulation may open the route to combinatorial studies, by employing different stimulation parameters in a fast, easily controllable and parallelized way, thus contributing to clarify the relationship between physical stimuli and differentiation.

## 2. Experimental section

### Cell isolation and culture

hASC populations were obtained from the waste tissues derived from aesthetic or prosthetic surgery performed at IRCCS Istituto Ortopedico Galeazzi, according to the procedure PQ 7.5.125, version 4. Written informed consent was obtained from all donors (6 females and 1 male, age range: 22–70 y/o). Briefly, hASC were isolated from subcutaneous adipose tissue following digestion with 0.75 mg $mL^{-1}$ type I collagenase (250 U $mg^{-1}$, Worthington Biochemical Corporation, Lakewood, NJ, USA) and filtering of the stromal vascular fraction. Cells were cultured in DMEM supplemented with 10% FBS (GE Healthcare, Life Science), 2 mM L-glutamine, 50 U $mL^{-1}$ penicillin and 50 μg $mL^{-1}$ streptomycin at 37 °C in a humidified atmosphere with 5% $CO_2$. Prior to their use, hASC were characterized for their clonogenicity, immunophenotype and multi-differentiative potential according to the international guidelines[27] and their features are summarized in the ESI† (Fig. S1). For each population, donor characteristics (age, gender and type of surgery) and the experiments in which cells were employed are summarized in the ESI† (Table S1).

### Sample preparation

Poly-3-hexyl-thiophene (P3HT, Sigma Aldrich) was dissolved in chlorobenzene (Carlo Erba) up to a final concentration of 20 mg $mL^{-1}$. The solution underwent overnight stirring at 65 °C to completely dissolve the powder. Glass substrates (VWR) were cleaned by sonication, upon subsequent rinses in water, acetone, and isopropanol (all from Sigma Aldrich). The polymer solution was spin coated on top of the glass substrates at 1500 rpm for 1 minute, up to a final thickness of about 150 nm. Both polymer samples and control glass substrates underwent oxygen plasma treatment (Diener Electronic-Femto) to increase their hydrophilicity and to improve cell adhesion, followed by a thermal sterilization process (2 hours at 120 °C). The absorbance scans were performed with a Lambda 1050 (PerkinElmer) UV/VIS/NIR spectrometer.

### Optical stimulation protocols

A home-made illuminator was designed *ad hoc*, to couple with a 6-well plate for cell culturing and to guarantee parallel illumination of polymer and control substrates within the cell incubator. Optical excitation was provided by a custom breadboard, comprising 6 green LEDs (SMB1N-525V-02; Roithner Laser Technik GmbH, Vienna, Austria) positioned to fit the central part of the wells. The emission wavelength peaks at 525 nm, and the LEDs carry a collimator lens reducing the emission angle to 22°. The light spot has a size of 1.13 $cm^2$ and the impinging power density is 200 μW $mm^{-2}$. The duty cycle and repetition rate of the stimulation were set through a custom control circuit, controlled by an Arduino Due (Arduino) microcontroller. Two different illumination

 

protocols were employed. In the first case, the duty cycle was 220 ms, with 20 ms illumination and 200 ms dark conditions (briefly indicated with the notation 20/200 throughout the following text). In the second case, the duty cycle was 4400 ms, with 400 ms illumination and 4000 ms dark conditions (briefly, 400/4000). Overall, the stimulation lasted for 6 hours in both cases.

### Cell proliferation assay

Material cytotoxicity was assessed by the Alamar Blue Cell Viability Reagent (Merck) assay. Cells were seeded on P3HT substrates, as well as on glass controls, in 48 wells plates at a density of $5 \times 10^3$ cells per $cm^2$. Cell proliferation was evaluated at 1, 4, 7, 11 and 14 days after incubation. For each time point, the growth medium was replaced with DMEM without phenol red (Sigma Aldrich) containing 10% of Alamar Blue. The samples were incubated again for 2 h 30 m at 37 °C in the dark. During Alamar Blue incubation, non-fluorescent resazurin is reduced to light emitting resorufin by cell respiration. After incubation, the solution was collected from the wells, and substituted with growth medium for further culturing. The solution was excited at 540 nm, and emission was measured at 600 nm with a Multimode Microplate Reader (Tecan, Spark 10M). The fluorescence values at different time points provide a growth curve, and the comparison with the control samples on glass offers qualitative information about the cell viability and proliferation capability.

### Confocal imaging

Undifferentiated hASC were plated on oxygen-plasma treated and thermally sterilized glass and P3HT-coated samples. 24 hours after plating, the cells were stained with Calcein AM (Merck, final concentration 2 μM) and Hoechst 33342 Fluorescent Stain (Merck, final concentration 1 μM) for cytosol and nuclei localization, respectively. Live imaging was performed with an Automated Fluorescence Microscope, equipped with a DAPI and FITC filtering sets (Olympus BX63). Image acquisition was carried out with Metamorph software (Molecular Devices). Images are reported as maximum intensity projection along the z-stack, processed with Fiji ImageJ software.

### Electrophysiology measurements

Electrophysiological recordings were performed using a patch-clamp setup (Axopatch 200B; Axon Instruments) coupled to a Nikon Eclipse Ti–S Inverted Microscope equipped with a solid-state LED stimulation system (Spectra III, Lumencor). Undifferentiated hASCs were plated on P3HT substrates, and the measurements were performed in whole-cell configuration with freshly pulled glass pipettes (resistance in the range 3–6 MΩ). The intracellular solution contained: 12 mM KCl, 125 mM K-gluconate, 1 mM $MgCl_2$, 0.1 mM $CaCl_2$, 10 mM EGTA, 10 mM Hepes, and 10 mM ATP (adenosine 5′-triphosphate)-$Na_2$. The extracellular solution contained: 135 mM NaCl, 5.4 mM KCl, 5 mM Hepes, 10 mM glucose, 1.8 mM $CaCl_2$, and 1 mM $MgCl_2$. Only single cells were selected for recordings. Membrane currents were low-pass filtered at 2 kHz and digitized with a sampling rate of 10 kHz (Digidata 1440A, Molecular Devices). Acquisition was performed with the pCLAMP 10 software (Axon Instruments).

### Calcium imaging

Undifferentiated hASCs were plated on both P3HT and glass control substrates. The cells were seeded at a density of $2 \times 10^4$ cells per $cm^2$ in complete culture medium. 24 hours after seeding, the cells underwent the optical stimulation protocol, lasting for 6 hours. Immediately after, the cells were stained with 1.5 μM Fluo-4 AM dye (Merck), diluted in extracellular solution (5 mM HEPES; 135 mM NaCl, 5.4 mM KCl, 1 mM $MgCl_2$, 1.8 mM $CaCl_2$, 10 mM glucose, all purchased from Sigma Aldrich; pH 7.4). The imaging experiments were carried out in the same extracellular solution, with a Nikon Eclipse Ti-S Inverted Microscope, equipped with a solid-state LED stimulation system (Spectra III, Lumencor); a FITC-filtering system (Thorlabs) was used to record only the emission wavelength of the probe. Three biological replicas were analysed, and for each replica an average of 60 cells was considered. Calcium-free measurements were carried out in calcium-free medium (10 mM HEPES; 150 mM NaCl, 3 mM $MgCl_2$, 5 mM EGTA, all purchased from Sigma Aldrich; pH 7.4). Two biological replicas were analysed. Images were recorded with MetaFluor 7.10.2.240 and analysed with OriginLab 2018.

### Alkaline phosphatase enzymatic assay

The activity of alkaline phosphatase (ALP), a widely accepted early marker of osteogenesis in bone-forming cells,[28] was assessed on cells grown for 14 days on glass or P3HT substrates, under either standard culture conditions or osteogenic stimuli (10 nM dexamethasone, 10 mM glycerol-2-phosphate, 150 mM L-ascorbic acid and 10 nM cholecalciferol, Sigma Aldrich). Briefly, cells were washed in phosphate buffer saline and lysed in 50 μL 0.1% Triton X-100 (Sigma Aldrich). ALP activity was assessed through a colorimetric assay based on the conversion of *p*-nitrophenyl phosphate into *p*-nitrophenol, as exhaustively described by Canciani *et al.*[29] The enzymatic activity (U) was inferred based on the amount of produced *p*-nitrophenol and the reaction time, then normalized with respect to each sample's protein concentration determined by BCA™ Protein Assay (Merck) and expressed as U $\mu g^{-1}$.

### Statistical analysis

All data are reported as mean ± standard error, after averaging the cells coming from the same biological replica. The different biological replicas have been separately reported. The Analysis of Variance (ANOVA) statistical analysis was carried out with OriginLab 2018 software, with alpha = 0.05. A *post hoc t*-student test was carried out. The statistical significance is reported as *, ** and ***, related to $p < 0.05$, $p < 0.01$ and $p < 0.001$, respectively.

## 3. Experimental results

### Light sensitive polymer substrates sustain *in vitro* proliferation of hASCs cultures

Poly(3-hexylthiophene-2,5-diyl) (P3HT) thin films, characterized by broad optical absorption in the blue/green visible range and

photoluminescence spectrum in the red (Fig. 1A), were previously, successfully employed as cell culturing substrates both for primary cells (hippocampal neurons,[30] astrocytes,[31] cardiac cells,[32] and endothelial cells[33]) and cell lines, as Human Embryonic Kidney cells (HEK293).[34] In existing reports by our and others' groups, no cytotoxic effects of conjugated polymer substrates on seeding and proliferation were observed.[19,35] However, their compatibility with undifferentiated stem cells was very rarely investigated.[33,36] In principle, the seeding and growth of undifferentiated cells may be affected by the surface topography of the polymer,[37] as well as by its hydrophobic character and chemical composition.[38,39] As a preliminary step, we thus checked whether the use of P3HT substrates affects adhesion and/or proliferation processes of undifferentiated hASCs. Fig. 1B shows good cell proliferation of hASCs on P3HT thin films, up to 14 days *in vitro*. No statistically significant difference is observed with respect to glass control samples. Fig. 1C and D are representative images of hASCs cultured on polymer and glass substrates: in both cases hASCs exhibit standard fibroblast or spindle-like morphology, with small cell bodies, long thin cytoplasmic processes, and wide nuclei. It is possible to appreciate the flatness of the hASC on the P3HT layer, indicating a strong adhesion to the polymer. Moreover, the staining further corroborates the evidence of a maintained cell viability on the polymer, as Calcein AM is converted to a green-fluorescent molecule only in the cytoplasm of viable cells by intracellular esterases. At last, P3HT biocompatibility was investigated also on hASCs undergoing osteogenic differentiation through the assessment of alkaline phosphatase (ALP) activity, an early marker of bone formation.[40] Fig. 1E shows the lack of interference of the P3HT substrate on the osteogenic commitment of cells grown for 14 days both in the absence (Ctrl) and in the presence (Osteo) of differentiative cues. Ultimately, no significant difference between the polymer or the glass substrate was ever observed, thus confirming that P3HT thin films support hASC seeding, adhesion, proliferation and osteogenic commitment.

### Bimodal modulation of hASC membrane potential by polymer photoexcitation

Due to their potentially important impact on cell proliferation and differentiation processes, ionic channel currents in undifferentiated hASCs have been previously characterized by whole-cell patch-clamp recordings. In more detail, the presence

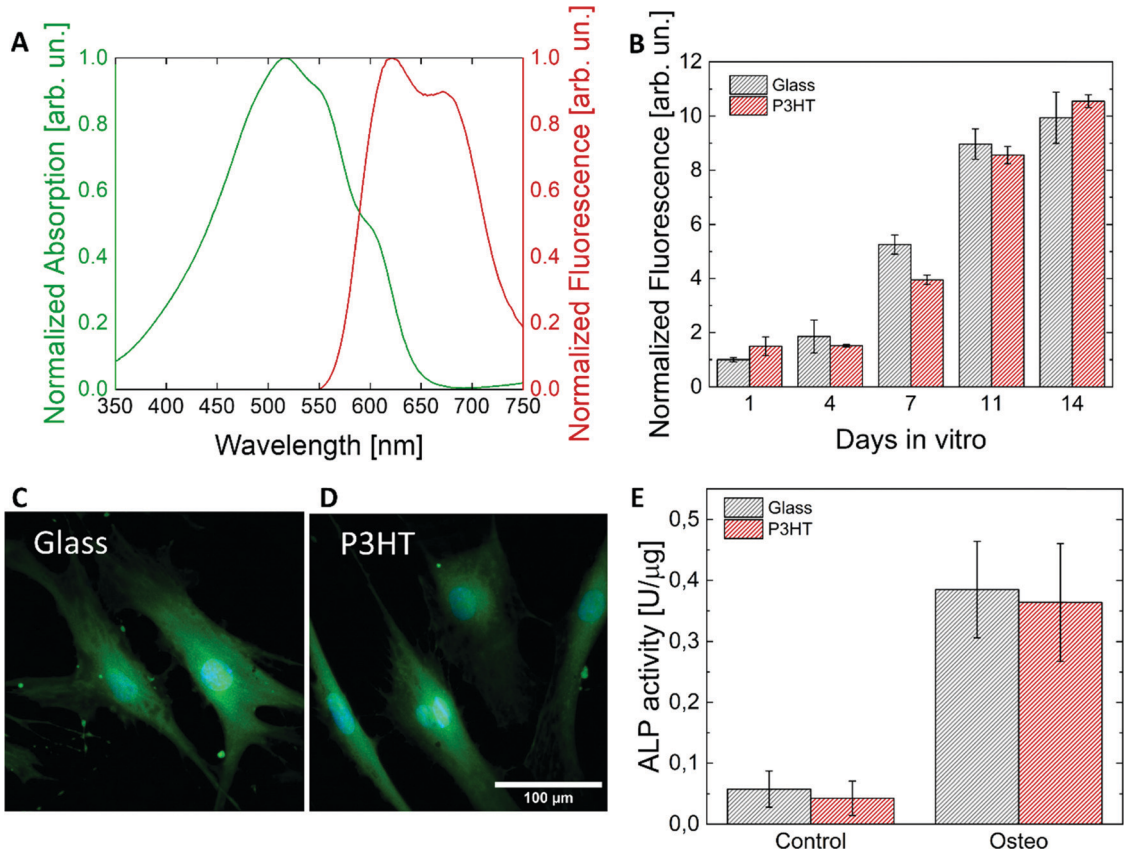


Fig. 1 P3HT supports hASCs seeding, proliferation and differentiation. (A) P3HT thin films absorption (green) and fluorescence (red) normalized spectra. (B) hASCs proliferation on glass and P3HT substrates (grey and red bars, respectively), as evaluated with the Alamar blue assay. Error bars represent the SEM. (C and D) Representative images of stem cells stained with Calcein and Hoechst on glass and P3HT substrates, respectively. Cells were imaged 48 h after division. (E) ALP activity of hASCs grown on glass and P3HT substrates (grey and red bars, respectively) under standard (Control) or osteogenic (Osteo) culture conditions. Data are derived from 3 independent experiments and are expressed as mean ± SEM. All the differences in panels (B) and (E) between cells on glass and P3HT are non-statistically significant.

 

of different types of currents was observed, out of which the slowly activating, delayed rectifier-like $K^+$ current was by far the predominant one. Conversely, the transient outward $K^+$ current, the $Ca^{2+}$ activated $K^+$ current and the transient inward $Na^{2+}$ current were observed only in smaller subpopulations of cells.[41] We carried out patch clamp measurements in voltage clamp configuration, to verify that the expected behaviour is preserved in the control cell cultures, seeded on glass slides, and to investigate the effect of concomitant optical excitation. A sketch of the experimental setup is shown in Fig. 2A. The system is coupled with a LED light source, which provides optical excitation in the green region of the spectrum, thus matching the optical absorption spectrum of the active polymer material (LED emission peak at 545 nm, power density 50 mW $mm^{-2}$). Membrane currents were elicited by a step-voltage protocol, consisting in 300 ms-long voltage steps between −100 mV and +60 mV, from a holding potential of −40 mV (Fig. 2B, inset). In line with literature reports, a delayed slowly activating positive current was observed, both in cells cultured on polymer substrates and on glass controls (Fig. 2B and C, respectively). On top of the voltage step protocol, continuous wave (CW) optical excitation was applied, lasting for 150 ms (represented in Fig. 2B and C by the green shaded area). Interestingly, the current recorded in polymer samples was significantly increased during photostimulation (up to +20% with the maximum positive applied potential, evaluated as the difference between the current values at the onset and the offset of the light stimulus), thus indicating effective stimulation of $K^+$ channels. The effect of light is reversible, since after switching off the light excitation, the transmembrane current rapidly decays to its equilibrium plateau before light onset. Conversely, current elicited in control samples by the voltage step protocol was not affected at all (Fig. 2C). Whole cell patch clamp measurements in current clamp configuration ($I$ = 0) confirm the effect of optical excitation mediated by polymer absorption (Fig. 2D). Upon photoexcitation, no variation of the cell membrane potential ($\Delta V_m$) is observed in glass control samples, thus indicating that light by itself does not alter the hASC physiological state (grey trace). Conversely, excitation of the P3HT polymer substrates deterministically leads to a variation of the resting membrane potential. In more detail, polymer light stimulation determines a depolarization signal ($\Delta V_m$ maximum, 0.27 ± 0.08 mV), followed by a larger hyperpolarization effect ($\Delta V_m$ immediately before light offset, −0.47 ± 0.11 mV). The combination of depolarizing and hyperpolarizing signals has already been observed in other cell models, including both excitable and non-excitable cells.[30,34] They were ascribed to a temperature-dependent variation of the cell membrane

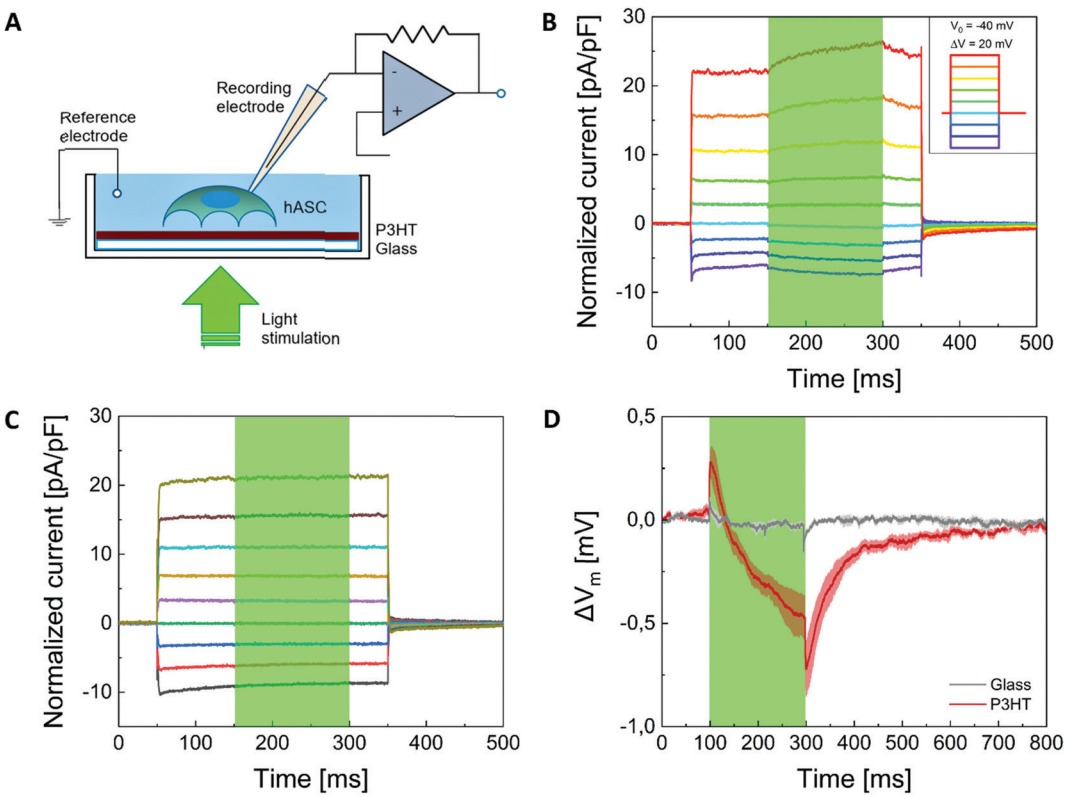


Fig. 2 Electrophysiology measurements. (A) Sketch of the setup and geometry used for patch clamp measurements. (B and C) Representative curves of voltage clamp measurements for hASCs on P3HT and glass substrates, respectively, at different potentials. One representative curve for each condition was selected, among the ones measured. (D) Representative curves of current clamp ($I$ = 0) measurements for hASCs on P3HT and glass as a control. The curves were obtained by averaging different measurements ($n$ = 4 on P3HT, $n$ = 3 on glass). The shaded error regions represent the SEM. The green shaded area represents the time window in which light stimulation was applied.

capacitance and resistance, respectively, and, in the case of primary neurons, elicitation of $K^+$ channels was proposed as the main pathway.[30] Furthermore, in endothelial cell models a similar effect was attributed to spatially-confined modulation of the transient receptor potential (TRP) vanilloid channel TRPV1, as mainly due to a photoelectrochemical process.[33,42] Interestingly, pH and temperature dependent channels, including canonical TRP (TRPC), melastatin TRP (TRPM), and tandem pore-class $K^+$ (TREK) channels, are also expressed in hASC, and they play critical roles in differentiation, migration and proliferation,[43,44] as much as $K^+$ channels.[45] However, future *ad hoc* pharmacological studies would be needed to unambiguously attribute the variation in the hASC membrane potential to specific ionic channels conductivity, and to unravel any influence on cell activity.

To the goals of the present work, in which we target chronic stimulation of hASC cultures during adhesion and proliferation stages, whole cell patch clamp studies allowed for identifying two timescales on which polymer excitation deterministically leads to a net positive (stimuli shorter than 20 ms) or negative (stimuli longer than 20 ms) variation of the cell membrane potential. This information has been at the base of the stimulation protocols selected for chronic excitation of hASC cultures, presented in the next section.

### P3HT actively modulates intracellular $Ca^{2+}$ dynamics

The involvement of $Ca^{2+}$ as a universal uniporter in cell physiological processes, such as growth, differentiation and proliferation, among others, led to insightful studies focused

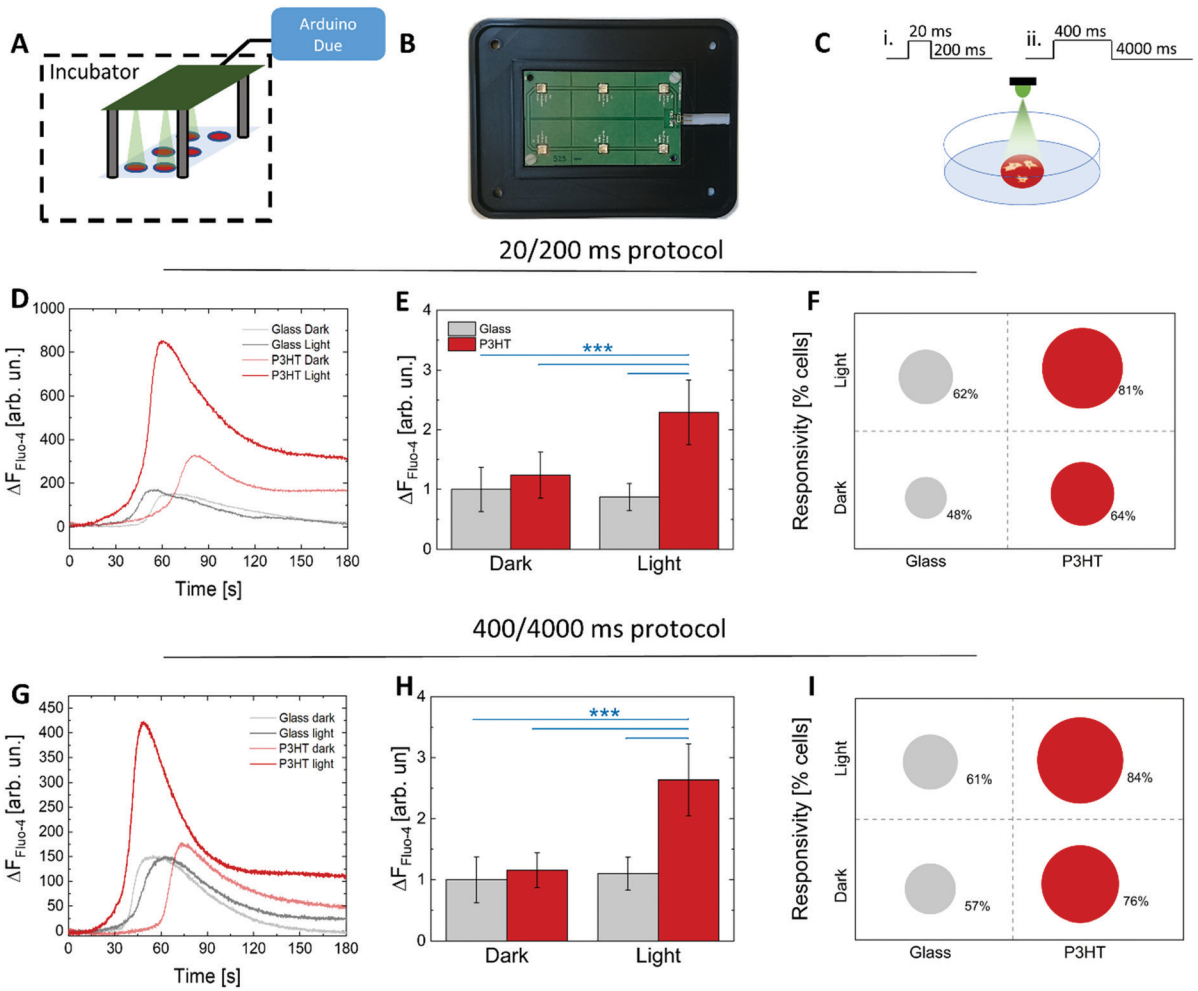


Fig. 3 $Ca^{2+}$ dynamics are modulated by P3HT photoexcitation. (A) Schematic representation of the home-made setup employed for the chronic stimulation of P3HT substrates. (B) Picture of the LED board used for stimulation. (C) Sketch reporting the illumination conditions for the living cells in the home-made setup. The cells are illuminated from the top ($P_d$ = 400 μW $mm^{-2}$) with two different illumination patterns. In one case, on a duty cycle of 220 ms, the light flashes for 20 ms (i). In the other case, the light flashes for 400 ms over a duty cycle of 4400 ms (ii). The two protocols are referred to as 20/200 and 400/4000, respectively. Panels (D–F) refer to the 20/200 stimulation protocol, while panels (G–I) refer to the 400/4000 stimulation protocol. (D and G) Representative $Ca^{2+}$ dynamics recorded at 20/200 and 400/4000 stimulation protocols, respectively, for cells grown on P3HT substrates upon illumination and in dark conditions (red and light red lines, respectively) and on glass substrates upon illumination and dark conditions (grey and light grey lines, respectively). (E and H) Average variation of $Ca^{2+}$ peaks in the different experimental conditions, after 20/00 and 400/4000 protocols stimulation, respectively. The statistical significance is reported for $p < 0.001$ (***), all other differences are not significantly different. (F and I) Cell responsivity evaluated for the two different illumination protocols, *i.e.* 20/200 and 400/4000. Details on how the responsivity was evaluated can be found in the ESI.†

 

on a cell specific $Ca^{2+}$ toolkit, aimed at controlling cellular behaviour through exogenous $Ca^{2+}$ modulation. Recent publications brought the attention to the $Ca^{2+}$ channels exhibited by undifferentiated human ASCs, and new findings revealed the involvement of this intracellular messenger on hASC differentiation.[46] To determine whether P3HT may act as an optically driven, modulating agent of hASC intracellular trafficking, we evaluated the effect of P3HT photostimulation on hASC $Ca^{2+}$ dynamics. We designed and implemented a home-made setup to optically, repeatedly stimulate the P3HT substrate in the $CO_2$ incubator, in cell culturing conditions. A simplified sketch and a picture of the LED board are reported in Fig. 3A and B, respectively. The culturing plate is coupled to a LED array, and the P3HT and glass substrates are illuminated from the top for 6 hours (Fig. 3C). According to the outcomes of the whole-cell patch clamp experiments, we employed two different illumination patterns, namely a 20 ms illumination/200 ms dark protocol, to maintain the membrane in a depolarized state, and a 400 ms illumination/4000 ms dark protocol, to maintain the membrane in a hyperpolarized state. The two protocols will be referred to from now onwards as 20/200 and 400/4000, respectively. Fig. 3D and G show representative $Ca^{2+}$ dynamics recorded after a 20/200 and 400/4000 illumination protocol, respectively, for cells cultured on P3HT and on glass substrates. Literature reports show that undifferentiated hASC present asynchronous $Ca^{2+}$oscillations, with some differences in the oscillation frequency from cell to cell (in the order, however, of about one $Ca^{2+}$ spike every 3–4 minutes), and a non-irrelevant subpopulation of cells which do not display at all spontaneous $Ca^{2+}$ oscillations.[47] In both P3HT and control glass substrates, oscillation frequency, as well as rise time, full-width half maximum, and decay dynamics are in line with existing reports.[47] Noticeably, however, hASCs grown on P3HT substrates and exposed to the 6 hour long illumination protocols 20/200 and 400/4000 exhibit remarkably higher $Ca^{2+}$ fluxes compared to those kept in dark conditions and to those grown on glass, either illuminated or not. The averaged amplitude variation of the $Ca^{2+}$ fluxes for $N = 100$ cells is reported in Fig. 3E and H for the 20/200 and the 400/4000 photoexcitation protocols, respectively. All the values were normalized to the average $Ca^{2+}$ amplitude of the control sample, *i.e.*, cells grown on glass and kept under dark conditions. The average $Ca^{2+}$ amplitude of cells grown on top of the P3HT samples exposed to illumination shows a statistically significant increase, by about $2.1 \pm 0.4$ and $2.7 \pm 0.7$ for the 20/200 and 400/4000 protocols respectively, with respect to all the other experimental conditions. Overall, these results unequivocally indicate that P3HT substrates and optical excitation in synergy, upon chronic optical stimulation, modulate the hASCs intracellular $Ca^{2+}$ trafficking.

As anticipated above, only a percentage of undifferentiated hASCs exhibit the signature of a $Ca^{2+}$ toolkit. In the absence of chemical cues or other differentiation stimuli, this has been associated to the fact that MSCs display $Ca^{2+}$ oscillations only during the phases G1 and S of the cell cycle, and it might be that not all the cells in the visualization area are in those phases of the cell cycle.[48] Importantly, $Ca^{2+}$ oscillations are known to increase the levels of cell cycle regulators such as cyclins A and E, and to control the cell cycle progression *via* the regulation of cyclin levels, amongst other mechanisms.[49] Thus, we quantitatively evaluated the percentage of cells exhibiting $Ca^{2+}$ spikes during the probing window (for further details see the ESI†), in photoexcited P3HT substrates and in control samples (Fig. 3F and I, for the 20/200 and 400/4000 protocols, respectively). We observe that the cells grown on P3HT or on glass substrates kept under dark conditions exhibit a low $Ca^{2+}$ responsivity, according to the results reported by Kawano *et al.*[47] Interestingly, however, the cells exposed to the light irradiation increase their responsivity, that reaches 81% and 84% in the case of cells grown on P3HT and exposed to the 20/200 and 400/4000 excitation protocols, respectively. The results are representative of one single biological population. Analogous results for experiments carried out on biological replicas can be found in the ESI† (Fig. S2).

Overall, these results indicate the opportunity to use optical cues to modulate the $Ca^{2+}$ toolkit in undifferentiated hASCs. Moreover, the light-triggered biophysical pathway activated at the cell/material interface and involving a substantial increase of $Ca^{2+}$ ion trafficking, may lead to regulation of cyclin levels, thus playing a role in the synchronization and acceleration of the cell cycle.

## $Ca^{2+}$ optical modulation is partially mediated by membrane channels

Spontaneous $Ca^{2+}$ oscillations are sustained by $Ca^{2+}$ channels and pumps at both the plasma membrane (PM) and the endoplasmic reticulum (ER). In fact, the $Ca^{2+}$ spikes can be originated either by the $Ca^{2+}$ entry from the external medium through the PM, or by the $Ca^{2+}$ release from the cell organelles, mainly the ER. The significant increase of intracellular $Ca^{2+}$ ion concentration observed upon photoexcitation prompted us to investigate what could be the main pathway active in the case of polymer samples. To this goal, we repeated the experiments presented in the previous section by employing a $Ca^{2+}$-free extracellular medium (Fig. 4). Data show that, while the removal of $Ca^{2+}$ ions does not have a significant impact on the control samples, neither for the 20/200 nor for the 400/4000 excitation protocol, it leads to a sizable reduction of the $Ca^{2+}$ fluorescence signal in the case of polymer samples (Fig. 4A and C). These results clearly indicate that the optical excitation of the polymer triggers $Ca^{2+}$ ion influx from the extracellular medium, which deterministically leads to the increase of intracellular $Ca^{2+}$ ion concentration, thus possibly involving a major contribution of $Ca^{2+}$ channels expressed on the PM. Interestingly, the capability of hASCs to express $Ca^{2+}$ signalling is also significantly decreased when $Ca^{2+}$ free extracellular medium is used, as compared to the controls, with a variation of 20% and 19% in the case of the 20/200 and 400/4000 light excitation protocols, respectively. The results are representative of a single population of undifferentiated stem cells; biological replicas are reported in the ESI† (Fig. S3).

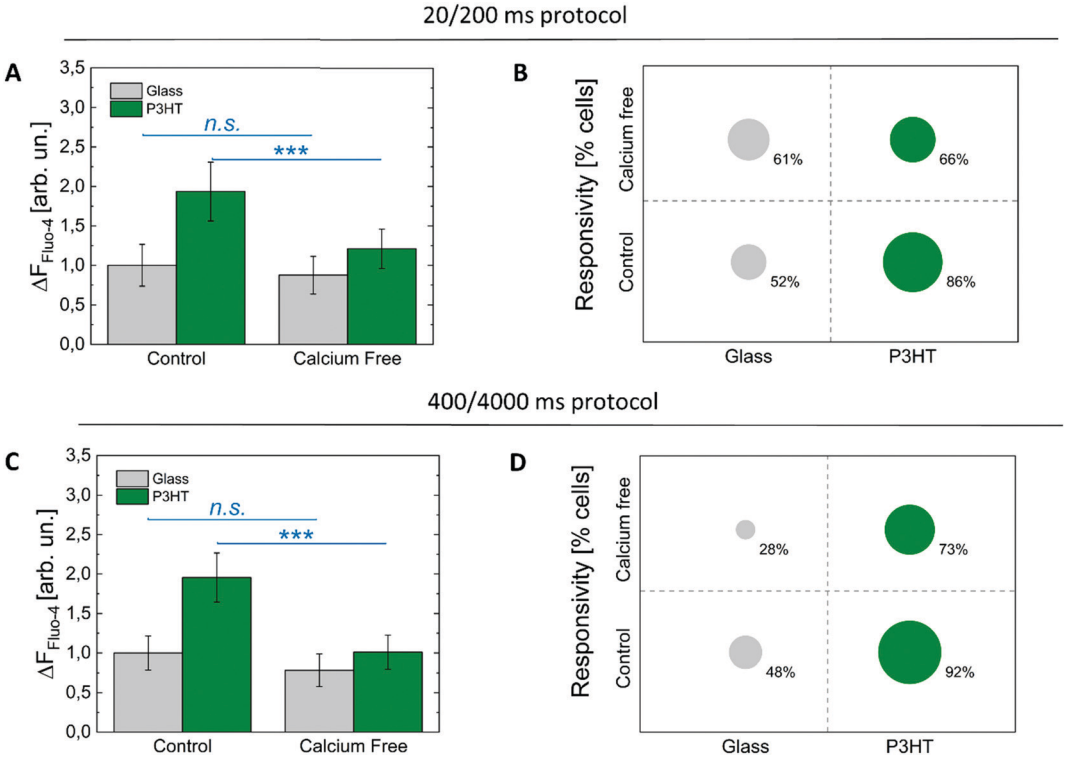


Fig. 4 Calcium recordings in $Ca^{2+}$ free medium. (A and C) Average $Ca^{2+}$ dynamics variation of cells grown on glass and P3HT substrates after 20/200 ms and 400/4000 ms protocols stimulation, in the control and $Ca^{2+}$ free media (grey and green bars, respectively). The statistical significance is reported for $p < 0.001$ (***) and for non-significant (n.s.). (B and D) Cell responsivity evaluated for the two different illumination protocols, respectively. Details on the responsivity evaluation are reported in the ESI.†

This result further corroborates the possible interplay between polymer excitation, $Ca^{2+}$ ion intracellular uptake and fine regulation of the cell cycle.

## 4. Discussion and conclusions

In this work we have reported the possibility of using physical stimuli, mediated by a light sensitive conjugated polymer thin film based on P3HT, to optically modulate key characteristics of undifferentiated hASCs under physiological conditions. More precisely, we have demonstrated that optical stimulation deterministically leads to a bimodal modulation of the cell membrane potential, characterized by a first depolarization effect (stimuli shorter than 20 ms), followed by a hyperpolarizing signal (stimuli longer than 20 ms, Fig. 2). The effect of light stimuli on $Ca^{2+}$ dynamics is instead univocal, irrespective of the stimuli time duration, and it consists of an increase in the intracellular $Ca^{2+}$ ion concentration, with a clear contribution of the extracellular $Ca^{2+}$ uptake processes. Interestingly, we observed that hASCs plated on the polymer thin films, and even more those exposed to photo stimulation, display enhanced $Ca^{2+}$ ion kinetics. This effect is partially diminished upon removal of the $Ca^{2+}$ ions from the extracellular solution (Fig. 3 and 4). Similar effects on the membrane potential driven by P3HT polymer optical excitation were previously observed, in several *in vitro* cell models, for instance in HEK-293T,[34] in primary neurons,[30] and in astrocytes.[31] In these cases, the bimodal modulation of the membrane potential was attributed to a photothermal transduction effect, consisting of (i) a variation of the cell capacitance, leading to a depolarization signal, at shorter times, combined with (ii) a variation of the cell ionic channels conductivity, at longer times, leading to the hyperpolarization signal. In the case of primary neurons, a clear role of $K^+$ channels was unequivocally demonstrated.[30] In endothelial colony forming cells seeded on P3HT thin films, the contribution of photo-activated electrochemical processes was also reported to play a key role in the modulation of the cell membrane potential, through activation of the multimodal transient receptor potential vanilloid channel TRPV1 expressed on the cell membrane.[33,50]

Quantifying and disentangling the different roles played by photogenerated electric fields, photoelectrochemical current and localized thermal effects, all possibly contributing to the observed membrane potential variation in hASCs, would require in depth biomolecular assays, and this will be addressed in a future work. Importantly, we notice here that the cell membrane potential, and more specifically a sustained depolarization signal, can have significant effects on the cell cycle. We thus hypothesize this is the cause of the observed higher responsivity of cells when plated on polymer substrates and exposed to chronic illumination protocols, thus continuously inducing sustained depolarization of the cell membrane. Conversely, the effects observed on $Ca^{2+}$ ion trafficking, both for short and for long light pulses, cannot be uniquely related to the variation of

 

the cell membrane potential, since in all cases we observed an increase of the $Ca^{2+}$ ion concentration. In addition, the process seems to be originated by a mechanism active at the interface between the cell membrane and the material, since we observe a role of the extracellular $Ca^{2+}$ uptake.

Interestingly, a sizable increase of intracellular $Ca^{2+}$ concentration, triggered by photoactivated polymer systems, was recently reported by Yuan and colleagues in the case of neuron-like PC-12 cells at 5 days *in vitro*.[21] The authors realized a tri-component material based on P3HT as the photoactive polymer, blended with polycaprolactone (PCL) and polypyrrole (PPY), and they observed, in line with our results, enhanced $Ca^{2+}$ concentration only in the case of illuminated samples containing P3HT, while no change was observed in control light-insensitive polymer samples (*i.e.*, comprising PCL and/or PPY, but not P3HT) or without photoexcitation. In other seminal works by Prof. Ramakrishna's group, P3HT:PCL nanofibers were reported to enhance cell proliferation of human dermal fibroblasts, possibly activated by an increase in cytosolic $Ca^{2+}$ concentration and downstream triggering of low molecular weight calmodulin protein.[51] A third example of P3HT-based substrates, promoting neurogenesis in human fetal neural stem cells, was reported by K. Yang and colleagues.[36] In this case, a cytosolic $Ca^{2+}$ increase after polymer photoexcitation was also qualitatively and preliminarily reported. In these reports, dealing with various cell models, a local electric field generated upon P3HT optical excitation was claimed as the origin of the cytosolic $Ca^{2+}$ increase.[52] Indeed, it has been reported that the exposure to an electromagnetic field, also in the absence of phototransduction processes driven by electrogenic materials, determines a sizable modulation of intracellular $Ca^{2+}$ ions, mediated by $Ca^{2+}$ ion permeabilization through the cell membrane.[48]

One should notice that additional mechanisms, possibly contributing to $Ca^{2+}$ modulation as well, were not considered at the moment, and, due to the lack of conclusive and quantitative control experiments, cannot be excluded. These include, among others, photothermal and photo-electrochemical transduction processes. In a recent work, we considered *in vitro* human endothelial precursors and we observed an increase in $Ca^{2+}$ concentration, which was unambiguously attributed to the generation of reactive oxygen species, at non-toxic concentration, and subsequent activation of multimodal TRPV1 channels.[42]

The data presented in this work on *in vitro* P3HT/hASC biohybrid interfaces exposed to optical excitation are not sufficient to unambiguously identify the biophysical and molecular pathways leading to the observed $Ca^{2+}$ increase. The following mechanisms may play a role, either independently or partially overlapped:

(i) P3HT-mediated photogeneration of ROS, at non-toxic concentrations;

(ii) Photo-thermal processes, and elicitation of temperature-dependent ionic channels, like TRP channels;

(iii) Stimulation of $Ca^{2+}$ gated ion channels, and in particular $K^+$ channels, which have been reported to induce a $Ca^{2+}$ ion increase in hASCs.

Additional work is currently on-going to elucidate the relative contribution of the mentioned mechanisms, or to identify alternative routes not considered so far, and will allow for more effective definition of critical parameters leading to hASCs physiology modulation.

In conclusion, we underline that both effects reported in this work, namely $Ca^{2+}$ concentration increase and membrane potential variation, are possibly related to a faster and/or more effective differentiation, as demonstrated in existing literature reports based on delivery of biochemical cues.[41,47,53] As compared to the latter approach, our strategy is minimally invasive, spatially confined and highly versatile, since the parameters of the light stimulation protocols can be optimized *ad hoc*. Importantly, this technique is easily applicable to any *in vitro* cell culture facility, in incubating conditions, with no need for expensive or bulky instrumentation, and in a remotely controlled way. These aspects are particularly intriguing since hASCs represent the most promising cell type for bone and cartilage regeneration in tissue engineering applications.[54] Moreover, the modulation of hASC physiological properties is expected to lead to a modification of their secretory profile, thus implying a change in the composition of the cell secretome, *i.e.* their conditioned medium (CM). Great interest has recently arisen toward the identification of specific cues able to modulate the plethora of vesicle-conveyed and soluble molecules secreted by MSCs. Indeed, a large part of MSC anti-inflammatory and immunomodulatory action does not rely on their multi-differentiative potential, whereas it depends on paracrine signalling. Therefore, in the last decade, the study of MSC CM has gained popularity[55–60] and this cell-free product has recently entered the first clinical trials. So far, multiple priming strategies have been tested to influence the release of specific factors by MSC. These include the use of cytokines, pharmacological and chemical agents, hypoxia, biomaterials and three-dimensional culture conditions.[61] The possibility to modulate MSC secretome by using optical stimulation and without altering the composition of the culture medium would be of great interest in the perspective of a future clinical use of this product. Moreover, the technique reported here may be extended without substantial changes to embryonic or induced pluripotent stem cells, which represent a widely targeted and promising model in stem cell research.

For these reasons, we believe that our results represent a useful and promising basis for further studies, aimed at investigating in detail the opportunity to use light for controlling the differentiation status of *in vitro* stem cells, and open the way to unprecedented tools in the field of regenerative medicine.

## Author contributions

M. R. A. and A. B. conceived, guided, and supervised the work. I. A. A. and L. M. designed the illumination protocol, implemented the experimental set up, realized polymer samples and carried out proliferation assays and fluorescence imaging and related analysis. I. A. A. and L. M. carried out $Ca^{2+}$ imaging

experiments and patch-clamp experiments and related analysis. S. N. and C. G. isolated, cultured and characterized hASC, and carried out ALP experiments and related analysis. All authors contributed to data interpretation. The manuscript was written through contributions of all authors. All authors have given approval to the final version of the manuscript.

## Funding sources

M. R. A. and I. A. A. acknowledge support by the European Research Council (ERC) under the European Union's Horizon 2020 research and innovation program 'LINCE', grant agreement no. 803621. MRA acknowledge support by the European Union's Horizon 2020 research and innovation program, H2020-FETOPEN-01-2018-2020 (FET-Open Challenging Current Thinking), 'LION-HEARTED', grant agreement no. 828984. The research was partially funded by the Italian Ministry of Health (grant number RC L1039, IRCCS Istituto Ortopedico Galeazzi) and University of Milan (grant number RV_LIB16ABRIN_M, Department of Biomedical, Surgical and Dental Sciences).

## Conflicts of interest

There are no conflicts to declare.

## Acknowledgements

The authors kindly thank Prof. Flavia Antonucci for her help in hASC patch clamp.

## References

1 R. E. B. Fitzsimmons, M. S. Mazurek, A. Soos and C. A. Simmons, *Stem Cells Int.*, 2018, **2018**, 1–16.
2 D.-T. Chu, T. Nguyen Thi Phuong, N. L. B. Tien, D. K. Tran, L. B. Minh, V. Van Thanh, P. Gia Anh, V. H. Pham and V. Thi Nga, *J. Clin. Med.*, 2019, **8**, 917.
3 W. Mende, R. Götzl, Y. Kubo, T. Pufe, T. Ruhl and J. P. Beier, *Cells*, 2021, **10**, 975.
4 J. Pak, J. Lee, N. Pak, Y. Pak, K. Park, J. Jeon, B. Jeong and S. Lee, *Int. J. Mol. Sci.*, 2018, **19**, 2146.
5 G. Yu, Z. E. Floyd, X. Wu, T. Hebert, Y.-D. C. Halvorsen, B. M. Buehrer and J. M. Gimble, in *LR Lloyd's Register*, ed. J. M. Gimble and B. A. Bunnell, Humana Press, Totowa, NJ, 2011, vol. 702, pp. 193–200.
6 J.-P. Stromps, N. E. Paul, B. Rath, M. Nourbakhsh, J. Bernhagen and N. Pallua, *BioMed Res. Int.*, 2014, **2014**, 1–7.
7 H. Shafaei and H. Kalarestaghi, *J. Cell. Physiol.*, 2020, **235**, 8371–8386.
8 P. Choudhary, A. Gupta and S. Singh, *J. Mol. Neurosci.*, 2021, **71**, 889–901.
9 Y. S. Choi, G. J. Dusting, S. Stubbs, S. Arunothayaraj, X. L. Han, P. Collas, W. A. Morrison and R. J. Dilley, *J. Cell. Mol. Med.*, 2010, **14**, 878–889.
10 A. Gelmi and C. E. Schutt, *Adv. Healthcare Mater.*, 2021, **10**, 2001125.
11 Y. Kong, J. Duan, F. Liu, L. Han, G. Li, C. Sun, Y. Sang, S. Wang, F. Yi and H. Liu, *Chem. Soc. Rev.*, 2021, **50**, 12828–12872.
12 J. Li, I. Mutreja, S. Tredinnick, M. Jermy, G. J. Hooper and T. B. F. Woodfield, *Mater. Sci. Eng., C*, 2020, **109**, 110562.
13 J. Zhang, M. Li, E.-T. Kang and K. G. Neoh, *Acta Biomater.*, 2016, **32**, 46–56.
14 M. Björninen, K. Gilmore, J. Pelto, R. Seppänen-Kaijansinkko, M. Kellomäki, S. Miettinen, G. Wallace, D. Grijpma and S. Haimi, *Ann. Biomed. Eng.*, 2017, **45**, 1015–1026.
15 T. Russo, V. Peluso, A. Gloria, O. Oliviero, L. Rinaldi, G. Improta, R. De Santis and V. D'Antò, *Nanomaterials*, 2020, **10**, 577.
16 L. Hao, L. Li, P. Wang, Z. Wang, X. Shi, M. Guo and P. Zhang, *Nanoscale*, 2019, **11**, 23423–23437.
17 S. Ding, P. Kingshott, H. Thissen, M. Pera and P.-Y. Wang, *Biotechnol. Bioeng.*, 2017, **114**, 260–280.
18 S. De Martino, S. Cavalli and P. A. Netti, *Adv. Healthcare Mater.*, 2020, **9**, 2000470.
19 E. Zeglio, A. L. Rutz, T. E. Winkler, G. G. Malliaras and A. Herland, *Adv. Mater.*, 2019, **31**, 1806712.
20 Y.-S. Hsiao, Y.-H. Liao, H.-L. Chen, P. Chen and F.-C. Chen, *ACS Appl. Mater. Interfaces*, 2016, **8**, 9275–9284.
21 B. Yuan, M. R. F. Aziz, S. Li, J. Wu, D. Li and R.-K. Li, *Acta Biomater.*, 2022, **139**, 82–90.
22 G. Jin, M. P. Prabhakaran and S. Ramakrishna, *Photochem. Photobiol.*, 2014, **90**, 673–681.
23 M. Berggren, E. D. Głowacki, D. T. Simon, E. Stavrinidou and K. Tybrandt, *Chem. Rev.*, 2022, **122**(4), 4826–4846.
24 A. Savva, A. Hama, G. Herrera-López, N. Gasparini, L. Migliaccio, M. Kawan, N. Steiner, I. McCulloch, D. Baran, H. Fiumelli, P. Magistretti, E. D. Głowacki and S. Inal, *bioRxiv*, 2022, DOI: 10.1101/2022.02.17.480608.
25 G. Tullii, A. Desii, C. Bossio, S. Bellani, M. Colombo, N. Martino, M. R. Antognazza and G. Lanzani, *Org. Electron.*, 2017, **46**, 88–98.
26 G. Tullii, F. Giona, F. Lodola, S. Bonfadini, C. Bossio, S. Varo, A. Desii, L. Criante, C. Sala, M. Pasini, C. Verpelli, F. Galeotti and M. R. Antognazza, *ACS Appl. Mater. Interfaces*, 2019, **11**, 28125–28137.
27 M. Dominici, K. Le Blanc, I. Mueller, I. Slaper-Cortenbach, F. Marini, D. S. Krause, R. J. Deans, A. Keating, D. J. Prockop and E. M. Horwitz, *Cytotherapy*, 2006, **8**, 315–317.
28 E. Wrobel, J. Leszczynska and E. Brzoska, *Cell. Mol. Biol. Lett.*, 2016, **21**, 26.
29 E. Canciani, C. Dellavia, L. M. Ferreira, C. Giannasi, D. Carmagnola, A. Carrassi and A. T. Brini, *J. Craniofac. Surg.*, 2016, **27**, 727–732.
30 P. Feyen, E. Colombo, D. Endeman, M. Nova, L. Laudato, N. Martino, M. R. Antognazza, G. Lanzani, F. Benfenati and D. Ghezzi, *Sci. Rep.*, 2016, **6**, 22718.
31 V. Benfenati, N. Martino, M. R. Antognazza, A. Pistone, S. Toffanin, S. Ferroni, G. Lanzani and M. Muccini, *Adv. Healthcare Mater.*, 2014, **3**, 392–399.

 

32 F. Lodola, V. Vurro, S. Crasto, E. Di Pasquale and G. Lanzani, *Adv. Healthcare Mater.*, 2019, **8**, 1900198.
33 F. Lodola, V. Rosti, G. Tullii, A. Desii, L. Tapella, P. Catarsi, D. Lim, F. Moccia and M. R. Antognazza, *Sci. Adv.*, 2019, **5**, eaav4620.
34 N. Martino, P. Feyen, M. Porro, C. Bossio, E. Zucchetti, D. Ghezzi, F. Benfenati, G. Lanzani and M. R. Antognazza, *Sci. Rep.*, 2015, **5**, 8911.
35 S. G. Higgins, A. Lo Fiego, I. Patrick, A. Creamer and M. M. Stevens, *Adv. Mater. Technol.*, 2020, **5**, 2000384.
36 K. Yang, J. Y. Oh, J. S. Lee, Y. Jin, G.-E. Chang, S. S. Chae, E. Cheong, H. K. Baik and S.-W. Cho, *Theranostics*, 2017, **7**, 4591–4604.
37 G. Abagnale, M. Steger, V. H. Nguyen, N. Hersch, A. Sechi, S. Joussen, B. Denecke, R. Merkel, B. Hoffmann, A. Dreser, U. Schnakenberg, A. Gillner and W. Wagner, *Biomaterials*, 2015, **61**, 316–326.
38 Z. Xing, J. Cai, Y. Sun, M. Cao, Y. Li, Y. Xue, A. Finne-Wistrand and M. Kamal, *Polymers*, 2020, **12**, 1453.
39 M. Lanniel, E. Huq, S. Allen, L. Buttery, P. M. Williams and M. R. Alexander, *Soft Matter*, 2011, **7**, 6501.
40 A. M. Osyczka and P. S. Leboy, *Endocrinology*, 2005, **146**, 3428–3437.
41 X. Bai, J. Ma, Z. Pan, Y.-H. Song, S. Freyberg, Y. Yan, D. Vykoukal and E. Alt, *Am. J. Physiol. Physiol.*, 2007, **293**, C1539–C1550.
42 S. Negri, P. Faris, G. Tullii, M. Vismara, A. F. Pellegata, F. Lodola, G. Guidetti, V. Rosti, M. R. Antognazza and F. Moccia, *Cell Calcium*, 2022, **101**, 102502.
43 M. V. Tarasov, P. D. Kotova, M. F. Bystrova, N. V. Kabanova, V. Y. Sysoeva and S. S. Kolesnikov, *Channels*, 2019, **13**, 36–47.
44 J. C. Henao, A. Grismaldo, A. Barreto, V. M. Rodríguez-Pardo, C. C. Mejía-Cruz, E. Leal-Garcia, R. Pérez-Núñez, P. Rojas, R. Latorre, I. Carvacho and Y. P. Torres, *Front. Cell Dev. Biol.*, 2021, **9**, 1–13.
45 S. Sundelacruz, M. Levin and D. L. Kaplan, *PLoS One*, 2008, **3**, e3737.
46 L. F. Mellor, M. Mohiti-Asli, J. Williams, A. Kannan, M. R. Dent, F. Guilak and E. G. Loboa, *Tissue Eng., Part A*, 2015, **21**, 2323–2333.
47 S. Kawano, S. Shoji, S. Ichinose, K. Yamagata, M. Tagami and M. Hiraoka, *Cell Calcium*, 2002, **32**, 165–174.
48 H. Hanna, F. M. Andre and L. M. Mir, *Stem Cell Res. Ther.*, 2017, **8**, 91.
49 R. R. Resende, A. Adhikari, J. da Costa, E. Lorençon, M. S. Ladeira, S. Guatimosim, A. H. Kihara and L. O. Ladeira, *Biochim. Biophys. Acta, Mol. Cell Res.*, 2010, **1803**, 246–260.
50 I. Abdel Aziz, M. Malferrari, F. Roggiani, G. Tullii, S. Rapino and M. R. Antognazza, *iScience*, 2020, **23**, 101091.
51 G. Jin, M. P. Prabhakaran, D. Kai, M. Kotaki and S. Ramakrishna, *Photochem. Photobiol. Sci.*, 2013, **12**, 124–134.
52 G. Polino, C. Lubrano, G. Ciccone and F. Santoro, *Front. Bioeng. Biotechnol.*, 2018, **6**, 1–6.
53 E. Pchelintseva and M. B. A. Djamgoz, *J. Cell. Physiol.*, 2018, **233**, 3755–3768.
54 G. S. Kronemberger, R. A. M. Matsui, G. A. S. C. Miranda, J. M. Granjeiro and L. S. Baptista, *World J. Stem Cells*, 2020, **12**, 110–122.
55 G. Amodeo, S. Niada, G. Moschetti, S. Franchi, P. Savadori, A. T. Brini and P. Sacerdote, *Brain, Behav., Immun.*, 2021, **94**, 29–40.
56 T. Montero-Vilchez, Á. Sierra-Sánchez, M. Sanchez-Diaz, M. I. Quiñones-Vico, R. Sanabria-de-la-Torre, A. Martinez-Lopez and S. Arias-Santiago, *Front. Cell Dev. Biol.*, 2021, **9**, 654210.
57 C. Giannasi, S. Niada, C. Magagnotti, E. Ragni, A. Andolfo and A. T. Brini, *Stem Cell Res. Ther.*, 2020, **11**, 521.
58 M. P. Benavides-Castellanos, N. Garzón-Orjuela and I. Linero, *Cell Regener.*, 2020, **9**, 5.
59 S. Niada, C. Giannasi, M. Gomarasca, D. Stanco, S. Casati and A. T. Brini, *Stem Cell Res.*, 2019, **38**, 101463.
60 A. T. Brini, G. Amodeo, L. M. Ferreira, A. Milani, S. Niada, G. Moschetti, S. Franchi, E. Borsani, L. F. Rodella, A. E. Panerai and P. Sacerdote, *Sci. Rep.*, 2017, **7**, 9904.
61 N. D. C. Noronha, A. Mizukami, C. Caliári-Oliveira, J. G. Cominal, J. L. M. Rocha, D. T. Covas, K. Swiech and K. C. R. Malmegrim, *Stem Cell Res. Ther.*, 2019, **10**, 131.